# A novel visible light-driven $TiO_2$ photocatalytic reduction for hexavalent chromium wastewater and mechanism

Baoxiu Zhao, Kaixin Zhang, Yue Huang, Qi Wang, Hao Xu, Yilin Wang, Jincheng Li, Tianwen Song, Wenxiang Xia and Jie Liu

## ABSTRACT

Titanium dioxide ($TiO_2$) photocatalyst was prepared with a sol-gel method and its characterizations were analyzed $TiO_2$ photocatalytic reduction of $Cr^{6+}$ was investigated in visible light irradiation and reduction mechanisms were calculated. Prepared $TiO_2$ is anatase with a bandgap of about 2.95 eV. Experimental results display that almost 100% of $Cr^{6+}$ is removed by visible light-driven $TiO_2$ photocatalytic reduction after 120 min when $Cr_2O_7^{2-}$ initial concentration is 1.0 mg·$L^{-1}$, $TiO_2$ dosage is 1.0 g·$L^{-1}$, and pH value is 3. In acidic aqueous solution, $HCrO_4^-$ is the dominant existing form of $Cr^{6+}$ and is adsorbed by $TiO_2$, forming a complex catalyst $HCrO_4^-/TiO_2$ with an increase in wavelength to the visible light zone, demonstrated by UV–Vis diffuse reflection spectroscopy. Based on X-ray photoelectron spectroscopy data, it can be deduced that $Cr^{6+}$ is adsorbed on the surface of $TiO_2$ and then reduced to $Cr^{3+}$ in situ by photoelectrons. Self-assembly of $HCrO_4^-/TiO_2$ complex catalyst and self-reduction of $Cr^{6+}$ in situ are the key steps to start the visible light-driven $TiO_2$ photocatalytic reduction. Furthermore, $TiO_2$ photocatalytic reduction of $Cr^{6+}$ fits well with pseudo-first-order kinetics and has the potential application to treat chemical industrial wastewater.

**Key words** | $Cr^{3+}$, $Cr^{6+}$, photocatalytic reduction, $TiO_2$, visible light

**Baoxiu Zhao** (corresponding author)
**Kaixin Zhang**
**Yue Huang**
**Qi Wang**
**Hao Xu**
**Yilin Wang**
**Jincheng Li**
**Tianwen Song**
**Wenxiang Xia**
**Jie Liu**
School of Environmental and Municipal Engineering,
Qingdao University of Technology,
Qingdao 266033,
China
E-mail: *zhaobaoxiu@tsinghua.org.cn*

## HIGHLIGHTS

- Cr(VI) is efficiently removed by visible light-driven $TiO_2$ photocatalytic reduction reaction.
- Photoinduced electrons are the major reductive substance for Cr(VI) removal.
- Adsorption, reduction in situ, and desorption are involved in reduction mechanism of Cr(VI).
- Photocatalytic reduction of Cr(VI) fits well with pseudo-first-order kinetics and rate constant is calculated.

## GRAPHICAL ABSTRACT

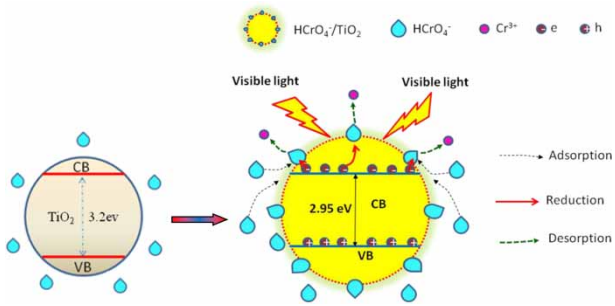




doi: 10.2166/wst.2021.116

## INTRODUCTION

Chromium pollutants mainly come from the industries of mining, metallurgy, electroplating, leather manufacture, bichromate, and chromium slag treatment (Zhang *et al.* 2017; Yang *et al.* 2018). However, they are used so widely that many tremendous environmental contaminations (Gheju & Balcu 2017; Ravindra & Mor 2019; Wang *et al.* 2020) are caused. $Cr^{6+}$ is the dominant existing form of chromium compounds and is easily absorbed by bodies. Many international investigations have found that some serious pathological lesions occur not only in the skin (Yu *et al.* 2018) but also in other organs caused when people are exposed to $Cr^{6+}$-rich environment for a long time (Guo *et al.* 2016; Yoshinaga *et al.* 2018). There are some methods for wastewater containing $Cr^{6+}$, such as adsorption or biosorption (Deveci & Kar 2013; Vendruscolo *et al.* 2017; Yao *et al.* 2017; Ayub *et al.* 2020), membrane separation (Habibi *et al.* 2015), electrolysis (Sarahney *et al.* 2012), and chemical reagents (Sheikhmohammadi *et al.* 2019). Adsorption is a convenient way for $Cr^{6+}$ removal (Gong *et al.* 2017), but the trace of absorbents should be noticed; otherwise, secondary pollution may be more serious. To avoid the potential risk of absorption, biosorption–biotransformation integrated processes where concentrated $Cr^{6+}$ is reduced to non-toxic $Cr^{3+}$ are developed (Jobby *et al.* 2018). However, the running environment and technical parameters are more strict than those of other technologies. Membrane separation can efficiently remove $Cr^{6+}$ from wastewater; however, membrane assembly is easily contaminated or blocked, and so how to efficiently, safely, and economically remove $Cr^{6+}$ becomes a research focus.

Semiconductor photocatalytic reaction is valued for its powerful redox ability, whether oxidation of most organics (Zhao *et al.* 2016) or reduction of variable valence heavy metal ions. Titanium dioxide ($TiO_2$) photocatalytic reduction for trace $Cr^{6+}$ has received researchers' attention (Testa *et al.* 2004; Yang *et al.* 2006) for its favorable chemical property, high stability, and low cost (Hoffmann *et al.* 1995). The absorption bandgap of pure $TiO_2$ ($E_g = 3.2$ eV) lies in the ultraviolet light zone ($\lambda = 1240/E_g = 385$ nm) (Fujishima *et al.* 2008), and it has no ability to oxidize or reduce pollutants in visible light irradiation. $TiO_2$ modification is a good way to achieve the visible light-driven photocatalytic reaction because the spectrum scope of modified $TiO_2$ transfers from the ultraviolet light region to the visible light zone. Modified $TiO_2$ photocatalyst and its application in wastewater treatments have been greatly developed recently. Doping non-ions elements and constructing heterojunctions are both effective methods to achieve $TiO_2$ photocatalytic performance in visible light irradiation. Chatterjee & Dasgupta (2005) discussed $TiO_2$ visible light-assisted degradation of organic pollutants and mechanism, and there is more research into $TiO_2$ photocatalytic degradation for organics in visible light irradiation. The bandgap of $TiO_2$ doped with elements such as N, F, S, and Bi or anions such as $OH^-$, $SO_4^{2-}$, and $ClO_4^-$ becomes narrow, producing a photoelectric response in visible light (Kerkez-Kuyumcu *et al.* 2015; Wang *et al.* 2017). Xu *et al.* (2019) prepared carbon dots (CDs)-modified N–$TiO_{2-x}$ nanocomposite to reduce $Cr^{6+}$ and obtained a satisfied efficiency in visible light irradiation. In addition, p–n junctions can also bring a red shift in the absorption spectrum, exhibiting a powerful visible light response. Magadevan *et al.* (2019) constructed a novel $TiO_2$–$Cu_2(OH)PO_4$ heterojunction catalyst and found that the composite catalyst exhibited high reduction efficiency of $Cr^{6+}$ because the bandgap narrowed from 3.2 eV to 2.6 eV. Dye-sensitized-$TiO_2$ also has photocatalytic reduction ability. Wu *et al.* (2013) prepared dye-sensitized $TiO_2$ to reduce $Cr^{6+}$ under visible light irradiation and found that $Cr^{6+}$ was reduced by photo electrons that diffuse from the dye-sensitized zone to the $TiO_2$ zone.

There are many investigations into reduction of $Cr^{6+}$ with $TiO_2$ ultraviolet photocatalysis (Zhou *et al.* 1993) or oxidation for organics with $TiO_2$ or modified $TiO_2$ (Asgari *et al.* 2021) or $TiO_2$-integrated process (Zhao *et al.* 2012, 2015, 2016); however, the study about direct reduction of $Cr^{6+}$ with pure $TiO_2$ in visible light is scarce. Our previous experiments have shown that in visible light irradiation, $Cr^{6+}$ is reduced to $Cr^{3+}$ by $TiO_2$ prepared by a sol-gel method. To investigate $TiO_2$ photocatalytic reduction of $Cr^{6+}$, process reactions and reduction mechanisms are analyzed in this work.

## EXPERIMENTAL

### Reagents and chemicals

Titanium butoxide, $H_2CrO_4$, $C_2H_5OH$, $CH_3COOH$, $K_2Cr_2O_7$, HCl, NaOH, and methanol were all analytical degree reagents and purchased from Tianjin Chemical Reagent Co. (China). High pure water (18.2 MΩ·$cm^{-1}$) was prepared via a water purification instrument (Unique-R20, Research Scientific Instruments Co. Ltd, China).

### Synthesis of $TiO_2$

$TiO_2$ was prepared via a sol-gel method where titanium butoxide ($Ti(OCH_2CH_2CH_2CH_3)_4$) was used as the precursor. Detailed process is as follows: 100 mL ethanol and 10 mL precursor were mixed together for 20 min at room temperature, forming a homogeneous mixture; 15 mL $H_2O$ and 4 mL $CH_3COOH$ were simultaneously added into the above-mentioned mixture, stirred for 40 min at a constant speed to obtain a mixture with a pH of about 4. The mixture was put into the oven and dried for a set time at 105 °C, to obtain the amorphous $TiO_2$. Finally, to reach the crystal phase transformation, amorphous $TiO_2$ was put into a box-type resistance furnace where a gradient temperature was preset. Temperature was raised from room temperature to 250 °C at a heating rate of 5 °C·min$^{-1}$ and kept for 1 h at 250 °C, and then increased from 250 °C to 600 °C at the same heating rate and maintained for 1 h at 600 °C.

### Characterization of as-prepared $TiO_2$

X-ray diffraction (XRD) pattern was monitored by a D/max RB system (Cu K$\alpha_1$ irradiation, $\lambda = 1.5406$ Å, voltage = 40 kV, current = 30 mA, scanning rate = 0.01°·s$^{-1}$, scanning range = 10–80°). Scanning electron microscope (SEM) images were obtained using a Fei Qunta Feg 250 microscope (accelerating voltage = 10 kV). UV–Vis diffuse reflectance spectrum (UV-DRS) was obtained using a UV–Vis diffuse reflectance spectrometer (LAMBDA 750, PerkinElmer) and scanning wavelength range from 200 to 800 nm. X-ray photoelectron spectroscopy (XPS) was controlled by an ESCALAB 250 Xi instrument (ThermoFisher Scientific, Al K$\alpha_1$ irradiation, h$\nu$ = 1486.6 eV, voltage = 12.5 kV, power = 250 W, pressure = $10^{-6}$–$10^{-7}$ Pa).

### $TiO_2$ photocatalytic reduction of $Cr^{6+}$

$TiO_2$ photocatalytic reduction of $Cr^{6+}$ was conducted in a cylindrical reactor equipped with a 150 W spherical xenon lamp (Shellett Photoelectric Technology Co. Ltd, China). A filter plate was used to remove ultraviolet light and 80 mW·cm$^{-1}$ irradiation intensity was measured using an illumination photometer. Then 200 mL of aqueous solution containing 1.0 mg·L$^{-1}$ $Cr_2O_7^{2-}$ and 1.0 g·L$^{-1}$ $TiO_2$ powder was transferred into the reactor and stirred at a speed of 100 r·min$^{-1}$ for 60 min, to obtain $Cr^{6+}$ adsorption equilibrium on the surface of $TiO_2$ and the inside of the reactor in a dark environment. After adsorption equilibrium, the light resource was turned on and photocatalytic reduction was started. Samples were removed from the same place in reactor at given time intervals and the concentration of $Cr^{6+}$ was analyzed using diphenylcarbazide colorimetric method controlled by a UV–Vis spectrophotometer (UV-1900, Shimadzu). Total chromium was analyzed with a graphite furnace atomic absorption spectroscopy (AA4590, Shimadzu).

## RESULTS AND DISCUSSION

### Characterizations of $TiO_2$

To determine the crystal phase of as-prepared $TiO_2$, XRD pattern was performed and results are shown in Figure 1(a)). Compared with the standard anatase $TiO_2$ (JCPDS: 89-4921), it is observed that the peaks at 2θ of 25.31°, 36.97°, 37.86°, 38.63°, 48.11°, 53.93°, 55.14°, 62.23°, 62.72°,

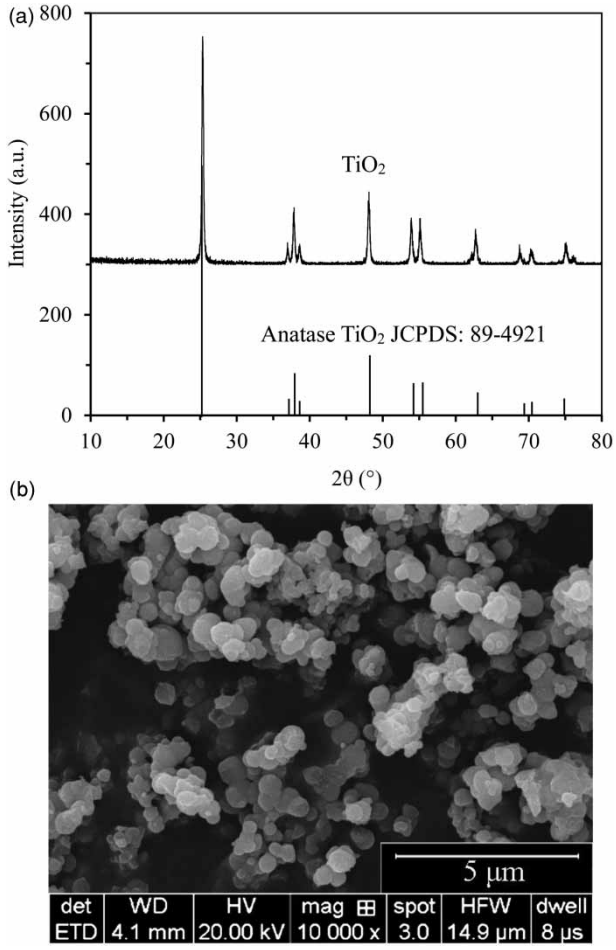


**Figure 1** | (a) XRD pattern of $TiO_2$; (b) SEM image of $TiO_2$.

68.75°, 70.28°, 75.13°, and 76.15° correspond to (101), (103), (004), (112), (200), (105), (211), (213), (204), (116), (220), (215), and (301) planes of anatase phase, suggesting that as-prepared $TiO_2$ is clear and perfect, which is in accordance with the research reported by Wang *et al.* (2021). SEM images of as-prepared $TiO_2$ are shown in Figure 1(b). It seems that $TiO_2$ looks like some uniform microspheres. The average size of as-prepared $TiO_2$ is about 78 nm, according to Debye–Scherrer formula ($D = K\lambda/\beta\cos\theta$), where K is a constant of 0.59, $\lambda$ is irradiation wavelength of 0.15406 nm, $\beta$ is half-maximum of (101) obtained via XRD software, and θ is the diffraction angle. Furthermore, the surface of $TiO_2$ is not smooth but layered, which is good for the adsorption and photocatalytic reduction of Cr(VI), compared to the smooth surface.

## Effects of $TiO_2$ dosage and $Cr_2O_7^{2-}$ concentration

The effect of $TiO_2$ dosage on photocatalytic reduction of $Cr^{6+}$ was investigated and results are displayed in Figure 2(a). It is observed that photocatalytic reduction of $Cr^{6+}$ increases initially and then decreases with the enhancement of $TiO_2$, and the optimum is 1.0 g·L$^{-1}$. The reason is that when $TiO_2$ dosage is lower than 1.0 g·L$^{-1}$, more $Cr^{6+}$ ions are adsorbed on the $TiO_2$ surface with the enhancement of catalyst dosage, resulting in high reduction; however, when the dosage is higher than 1.0 g·L$^{-1}$, the homogeneous solution becomes murky with the increase in catalyst dosage, leading to a reflection of light, meaning that only the surface layer $Cr^{6+}$ aqueous solution receives light irradiation, resulting in low photocatalytic reduction efficiency.

The effect of $Cr_2O_7^{2-}$ concentration on photocatalytic reduction of $Cr^{6+}$ was studied and results are shown in Figure 2(b). It can be seen that reduction efficiency decreases with the enhancement of $Cr_2O_7^{2-}$ concentration. Reduction of $Cr^{6+}$ climbs to 98% at 90 min when $Cr_2O_7^{2-}$ initial concentration is 0.5 mg·L$^{-1}$; however, it is only 24% when the $Cr_2O_7^{2-}$ initial concentration is 5.0 mg·L$^{-1}$. The decline of reduction is mainly caused by light scattering. The higher the $Cr_2O_7^{2-}$ initial concentration, the darker the aqueous solution becomes, and then the $Cr_2O_7^{2-}$ anions participating in photocatalytic reduction reduces for the serious scattering of visible light.

## Effect of pH

The effect of pH on photocatalytic reduction of $Cr^{6+}$ was studied under visible light and results are displayed in

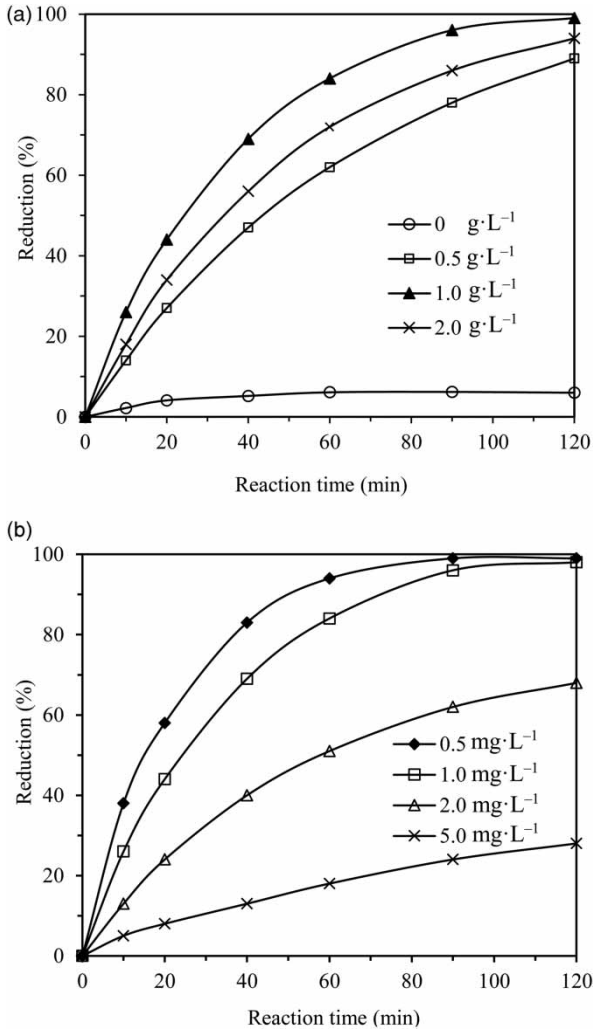


**Figure 2** | (a) Effect of $TiO_2$ dosage on photocatalytic reduction of $Cr^{6+}$ in the presence of air bubbles, where $[Cr_2O_7^{2-}] = 1.0$ mg·L$^{-1}$, pH = 3, $P = 150$ W; (b) effect of $Cr_2O_7^{2-}$ concentration on photocatalytic reduction of $Cr^{6+}$ in the presence of air bubbles, where $[TiO_2] = 1.0$ g·L$^{-1}$, pH = 3.0, $P = 150$ W.

Figure 3(a). It is observed that photocatalytic reduction efficiency decreases with the enhancement of pH value. In $TiO_2$ photocatalytic reduction of $Cr^{6+}$, pH not only affects the charge property of $TiO_2$ but also influences the existing form of $Cr^{6+}$ species. Acharya *et al.* (2018) found that the existing form of $Cr^{6+}$ strictly depends on pH value: $H_2CrO_4$ molecule (pH < 2), $HCrO_4^-$ (2 < pH < 7) and $Cr_2O_7^{2-}$ (pH >7). The isoelectric point of photocatalyst varies depending on preparation conditions, and is particularly affected by pH value (Gumy *et al.* 2006). The isoelectric point of as-prepared $TiO_2$ was tested using an electrochemical method controlled by a zeta potentiometer and was found to be about 5. The surface of $TiO_2$ is positively charged when the pH value is lower than 5 and

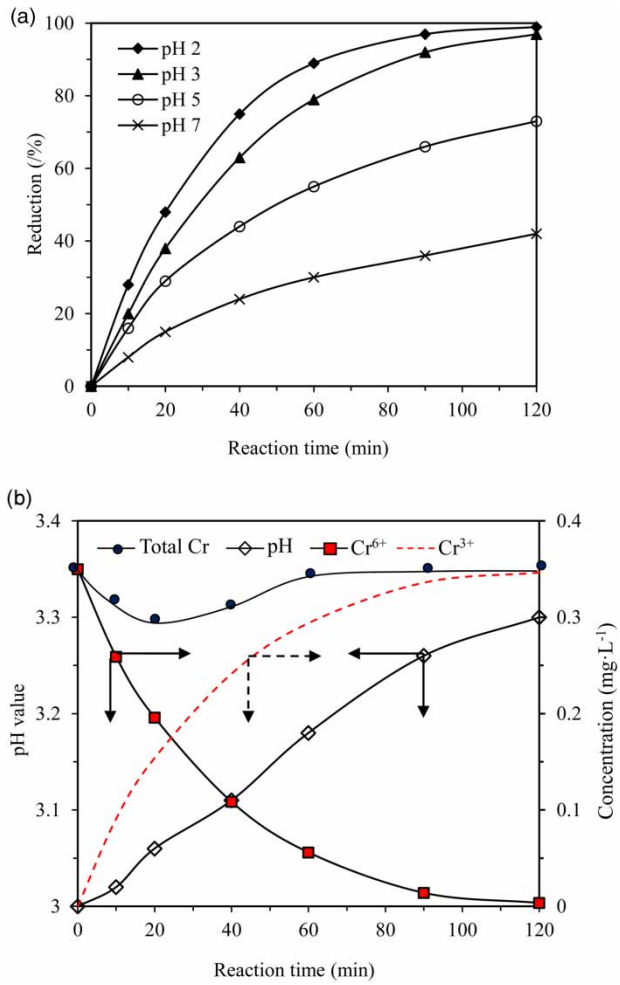


**Figure 3** | (a) Effect of pH values on photocatalytic reduction of $Cr^{6+}$ in the presence of air bubbles; (b) the changes of pH, concentration of $Cr^{6+}$, and $Cr^{3+}$ during photocatalytic reduction, where $[TiO_2] = 1.0\ g{\cdot}L^{-1}$, $[Cr_2O_7^{2-}] = 1.0\ mg{\cdot}L^{-1}$, $P = 150$ W.

negatively charged when the pH value is higher than 5. In $TiO_2$ photocatalytic reduction, the main form of $Cr^{6+}$ is $HCrO_4^-$ when the pH value ranges from 2 to 5. In this situation, the $TiO_2$ surface is positive, and more $HCrO_4^-$ anions are adsorbed onto the $TiO_2$ surface due to coulomb attraction forces when the pH value declines gradually. The adsorbed $HCrO_4^-$ ions are then reduced to $Cr^{3+}$ in situ by reductive substances. When the pH value increases from 5 to 7, the dominant existing form of $Cr^{6+}$ is still $HCrO_4^-$; however, the negative charge property of the $TiO_2$ surface becomes stronger, which results in the adsorption of $HCrO_4^-$ anions on the catalyst surface and so the photocatalytic reduction declines. Adsorption is a key step for photocatalytic reactions – the stronger the adsorption, the higher the photocatalytic reduction efficiency.

$HCrO_4^-$ ions are reduced to $Cr^{3+}$ in $TiO_2$ photocatalytic reduction, consuming lots of hydrogen ions, as the following equations demonstrates:

$$3e^- + 7H^+ + HCrO_4^- = Cr^{3+} + 4H_2O \quad \text{(R1)}$$

Figure 3(b) records the changes of pH value and $Cr^{6+}$ concentration. From this figure, it can be seen that the pH value enhances from 3.0 to 3.3 and the $Cr^{6+}$ concentration declines from 0.35 to 0.017 $mg{\cdot}L^{-1}$ after 120 min. The concentration of generated $Cr^{3+}$ ions is 0.35 $mg{\cdot}L^{-1}$ at the same reaction time, theoretically. In fact, the actual $Cr^{3+}$ may be lower than the theoretically concentration because some produced $Cr^{3+}$ is still adsorbed on the $TiO_2$ surface, as shown by XPS analysis. On the other hand, dissolved $Cr^{3+}$ may be precipitated to $Cr(OH)_3$ by $OH^-$ anions if the mathematical product of $Cr^{3+}$ and $(OH^-)^3$ is higher than the solubility of $Cr(OH)_3$ ($K_{sp} = 6.31 \times 10^{-31}$), as in the following chemical reaction:

$$Cr^{3+} + 3OH^- \rightleftharpoons Cr(OH)_3 \quad \text{(R2)}$$

In this experiment, it is presumed that all $HCrO_4^-$ ions are reduced to $Cr^{3+}$ and released into solution, the maximum concentration of $Cr^{3+}$ reached is at $2/294 \times 10^{-3}$ $mol{\cdot}L^{-1}$ (initial concentration of $K_2Cr_2O_7$ is 1.0 $mg{\cdot}L^{-1}$). At the same time, if the $H^+$ ions are assumed to be about $2 \times 7/294 \times 10^{-3}$ $mol{\cdot}L^{-1}$ according to Equation (R1), then the $OH^-$ concentration increases to $10^{-14}/(10^{-3} - 2 \times 10^{-3} \times 7/294)$ $mol{\cdot}L^{-1}$ according to the ion product constant of water. The product of $Cr^{3+}$ and $(OH^-)^3$ is $7 \times 10^{-39}$, which is much lower than $6.31 \times 10^{-31}$. This means that $Cr^{3+}$ cannot be precipitated in the form of $Cr(OH)_3$ in this experiment.

## Effect of atmospheres and scavengers

Effects of $N_2$, $O_2$, and air bubbles on $TiO_2$ photocatalytic reductions were studied and the results are shown in Figure 4(a). It is observed that the order of reduction ability of $Cr^{6+}$ is $N_2 >$ air $> O_2$, suggesting that $N_2$ is positive for reduction and $O_2$ is negative for it. This is probably because the amount of $O_2$ molecules consume photoinduced electrons to produce a superoxide radical $\cdot O_2^-$, displayed in the following reaction:

$$O_2 + e \rightarrow \cdot O_2^- \quad \text{(R3)}$$

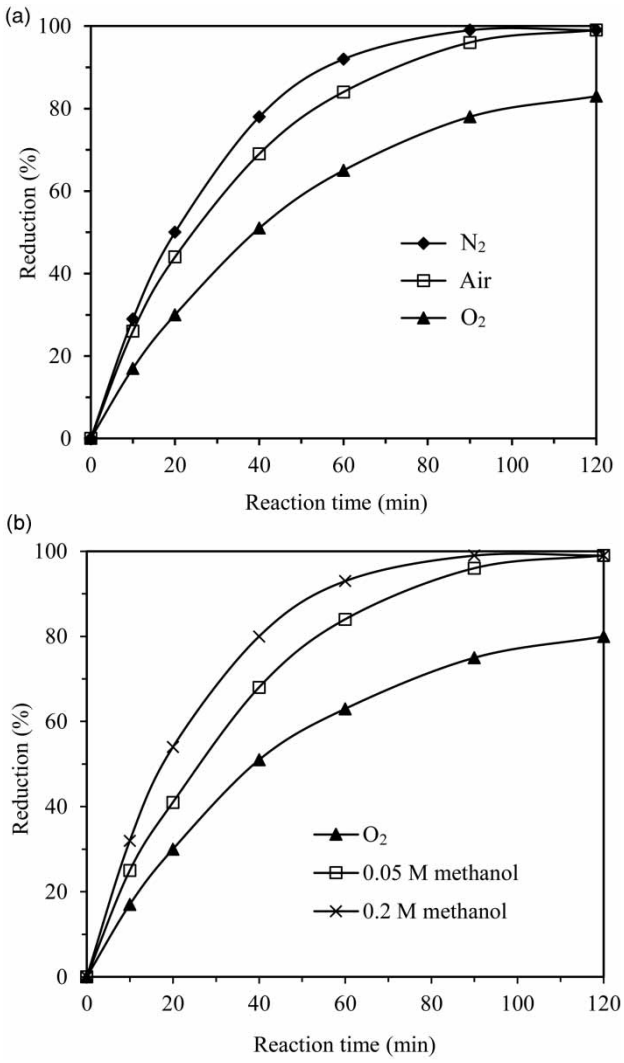


**Figure 4** | (a) Effect of $N_2$, $O_2$, and air bubbles on photocatalytic reduction of $Cr^{6+}$; (b) effect of scavengers on photocatalytic reduction of $Cr^{6+}$, where $[TiO_2] = 1.0\ g{\cdot}L^{-1}$, $[Cr_2O_7^{2-}] = 1.0\ mg{\cdot}L^{-1}$, pH = 3, $P = 150$ W.

The production of $\cdot O_2^-$ aggravates a tense competition between $O_2$ and $Cr^{6+}$ with photoinduced electrons, and only some of the photoinduced electrons are involved in the reduction of $Cr^{6+}$, inhibiting photocatalytic reduction efficiency. On the contrary, bubbling $N_2$ can greatly drive dissolved $O_2$ which is an effective photoinduced electron scavenger from aqueous solution, and as a result, more photoinduced electrons can take part in the reduction of $Cr^{6+}$ in this situation, compared with those in $O_2$ or air atmospheres. In fact, oxidation–reduction is a concurrent reaction in the $TiO_2$ photocatalytic process. In this work, $TiO_2$ photocatalytic reduction conducted by photoinduced electrons was used to treat $Cr^{+6}$. A partial oxidation reaction caused by photoinduced holes or hydroxyl radicals occurs, which consumes a lot of photoinduced electrons if there is no additional scavenger of holes, leading to low photocatalytic efficiency.

To inhibit the recombination of photoinduced carriers and deduce photocatalytic reduction pathway, methanol acting as a scavenger of holes was added to system. The influence of methanol on $TiO_2$ photocatalytic reduction was determined and the results are displayed in Figure 4(b). It is observed that the photocatalytic reduction efficiency of $Cr^{6+}$ increased and it increases with an increase in methanol dosage. Well known, photoinduced holes are easily captured by methanol (Gumy *et al.* 2006), hence more photoinduced electrons can participate in the reduction of $Cr^{+6}$ instead of recombination of carriers, compared with those in the absence of methanol, which verifies that $Cr^{6+}$ is removed via photocatalytic reduction channel.

## Photocatalytic reduction mechanism

The $HCrO_4^-$ anion is the dominant existing form when the pH is between 2 and 7. In this situation, adsorption of $HCrO_4^-$ spontaneously happens on the surface of $TiO_2$, forming a narrow bandgap $HCrO_4/TiO_2$ complex catalyst, which is proven by UV–Vis DRS analysis. Photoinduced electrons are generated on the $HCrO_4^-/TiO_2$ conduction band in visible light irradiation and are involved in the reduction of $Cr^{6+}$. To verify this hypothesis, XPS and UV–Vis DRS were both conducted and the results are shown in Figure 5. Figure 5(a) displays the XPS spectra of three samples. The first sample is as-prepared $TiO_2$ powder, named as $TiO_2$; the second is $TiO_2$ powder which is soaked in $1.0\ mg{\cdot}L^{-1}$ $Cr_2O_7^{2-}$ aqueous solution for 1 h in dark and then dried at 100 °C, named as $TiO_2$ before reaction; and the third is $TiO_2$ powder which is recovered from the reduction system after 120 min, named as $TiO_2$ after reaction. It is apparent that there are three characteristic peaks in the spectrum of $TiO_2$ with binding energies of 530.2 eV, 459.5 eV, and 285.7 eV, and they are assigned to O1s, Ti2p, and C1s elements, respectively. The peak of C1s is possibly caused by pollution. It is found that Cr2p intensity in the spectrum of $TiO_2$ before reaction (blue line) is stronger than that of $TiO_2$ (black line), suggesting that some $HCrO_4^-$ ions are adsorbed onto the $TiO_2$ surface in dark conditions. However, it is surprising that the Cr2p peak almost disappears in the spectrum of $TiO_2$ after reaction (red line), revealing that adsorbed $HCrO_4^-$ ions are reduced under visible light irradiation. Three continuous steps including adsorption, reduction, and desorption are involved in the reduction of $Cr^{6+}$. These steps continue until almost all $HCrO_4^-$ anions are reduced.

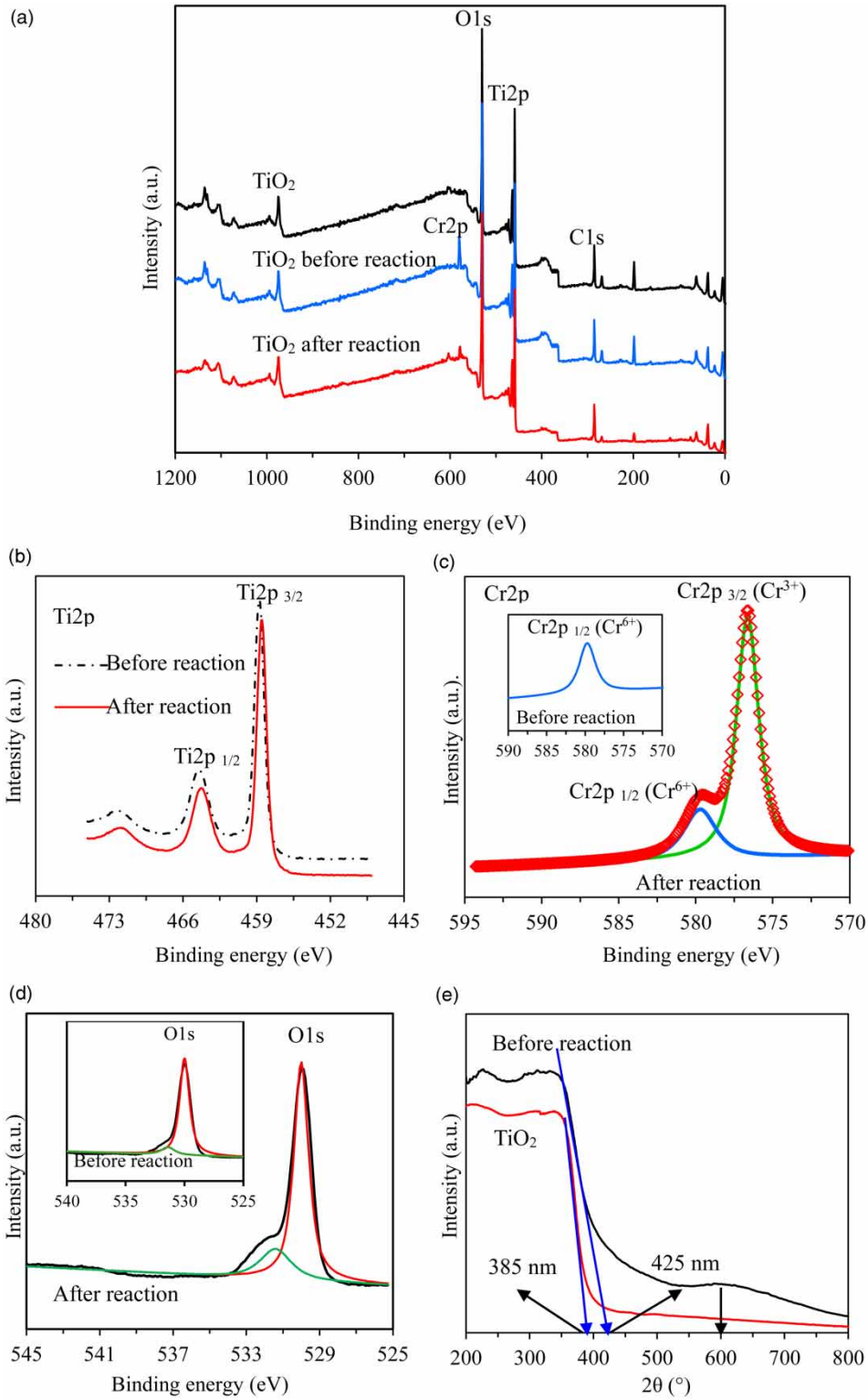


**Figure 5** | (a) XPS spectra of three samples ($TiO_2$, $TiO_2$ before, and $TiO_2$ after reaction); (b) Ti2p XPS spectrum and separation peak at the binding energy of 459.5 eV for two samples ($TiO_2$ before and $TiO_2$ after reaction); (c) Cr2p XPS spectrum and separation peak at the binding energy of 579.7 eV for the sample ($TiO_2$ after reaction), and the inset is the Cr2p XPS spectrum of the sample ($TiO_2$ before reaction); (d) O1s XPS spectra and separation peak at the binding energy of 530.2 eV for two samples of $TiO_2$ after reaction and $TiO_2$ before reaction (the inset picture); (e) UV–Vis diffuse reflectance spectra of $TiO_2$ and $TiO_2$ before reaction.

The peak of Ti2p binding at 459.5 eV was fitted using XPS software and results are shown in Figure 5(b). One peak appears at the binding energy of 464.4 eV which is caused by $Ti2p_{1/2}$ and the other appears at 458.8 eV which is caused by $Ti2P_{3/2}$. It is found that $Ti^{4+}$ is the only chemical form during the whole photocatalytic reduction, demonstrating that $TiO_2$ keeps a good structural stability. The fitting of Cr2p binding at 579.7 eV was also analyzed and results are shown in Figure 5(c). The spectrum of Cr2p marked with red diamonds is divided into two individual spectra marked with green and blue curves, respectively. The blue line represents the spectrum of $Cr2p_{1/2}$ and it belongs to $Cr^{6+}$ with a characteristic peak at 579.7 eV. The green line represents the spectrum of $Cr2p_{3/2}$ and is assigned to $Cr^{3+}$ with the characteristic peak at 576.6 eV. It is concluded that $Cr^{3+}$ is the only reductive product. At the same time, the fitting of Cr2p in the spectrum before photocatalytic reaction was simulated, but there is only one $Cr2p_{1/2}$ peak caused by $Cr^{6+}$, shown in Figure 5(c). This shows that $HCrO_4^-$ is intitially adsorbed on the surface of $TiO_2$ before photocatalytic reaction and is then reduced in situ to $Cr^{3+}$ in visible light irradiation. The quantities of $Cr^{6+}$ and $Cr^{3+}$ adsorbed on the $TiO_2$ surface are calculated and exported using software. Molar ratio of $Cr^{6+}$:$Cr^{3+}$ is about 1:4, indicating that $HCrO_4^-$ is reduced to $Cr^{3+}$ and that $Cr^{3+}$ ions still adsorb on the surface of $TiO_2$ catalyst. Figure 5(d) displays the fitting of O1s spectra in two samples of $TiO_2$ after and before reaction (inset figure), respectively. It is observed that O1s binding at 530.2 eV can be divided into two peaks. One peak binding at 530.0 eV (red curve) is assigned to the lattice oxygen coming from $TiO_2$ and $HCrO_4^-$, and the other binding at about 531.4 eV (green curve) probably belongs to hydroxyl oxygen coming from the chemical adsorption of oxygen, which is in accordance with the conclusion by Yang *et al.* (2006). It is obvious that the hydroxyl oxygen is higher on the $TiO_2$ surface after the reaction than before reaction, proving that $O_2$ or $OH^-$ or produced $\cdot O_2^-$ adsorbs on the $TiO_2$ surface during photocatalytic reduction. Figure 5(e) shows the absorption bandgap of pure $TiO_2$ and $TiO_2$ before photocatalytic reaction. The absorption of pure $TiO_2$ focuses on the ultraviolet zone and that of $TiO_2$/$HCrO_4^-$ increases to visible light scope, proving that $TiO_2$/$HCrO_4^-$ can produce photoinduced carriers irradiated by visible light.

Based on the above analysis, visible light-driven $TiO_2$ photocatalytic reduction of $Cr^{6+}$ was explored. The mechanism involves four major pathways: (1) adsorption of $HCrO_4^-$ on the surface of $TiO_2$; (2) production of photoinduced electrons under visible light irradiation; (3) reduction of $Cr^{6+}$ to $Cr^{3+}$ by photoinduced electrons; and (4) desorption of $Cr^{3+}$. The cycle of adsorption → reduction → desorption continues until almost all the $HCrO_4^-$ is reduced.

### Life span, kinetics and application

$TiO_2$ was reused eight times under the same experimental conditions and the results are shown in Figure 6(a). It is observed that the $TiO_2$ photocatalytic reduction efficiency does not decrease with recycled times, showing that $TiO_2$ has a satisfied structural stability and a potential application for use in wastewater treatment. Photocatalytic reduction kinetics of $Cr^{6+}$ with $TiO_2$ was investigated and results are shown in Figure 6(b) and 6(c). The photocatalytic reduction fits well with pseudo-first-order kinetics when $Cr_2O_7^{2-}$ initial concentration ranges from 0.5 to 5.0 $mg{\cdot}L^{-1}$, and rate constants decrease with the enhancement of $Cr_2O_7^{2-}$ initial concentration. The functional relationship between first-order kinetic rate constants and $Cr_2O_7^{2-}$ initial concentration was simulated and shown in Figure 6(c). Pseudo-first-order kinetics constant ($k$) can be described as: $k = 0.023\ C^{-1.42}$, where $C$ is the $Cr_2O_7^{2-}$ initial concentration. Hence, we can obtain the corresponding $k$ value at a certain $Cr_2O_7^{2-}$ initial concentration according to this simulation.

To investigate the application of $TiO_2$ photocatalytic reduction in real industrial wastewater containing $Cr^{6+}$, a small-scale static test was carried out in the same reactor. Properties, including $Cr_2O_7^{2-}$ initial concentration and pH of chemical wastewater, are listed in Table 1, and experimental results are shown in Figure 6(d). It is observed that removal efficiencies of $Cr^{6+}$ in the simulation experiment and small-scale static test are 100% and 93%, respectively, suggesting that $TiO_2$ photocatalytic reduction can be used to treat wastewater containing $Cr^{6+}$. The slight decline of $Cr^{6+}$removal may be caused by co-existing ions in chemical wastewater.

## CONCLUSIONS

Almost 100% of $Cr^{6+}$ is reduced to $Cr^{3+}$ in situ by visible light-driven $TiO_2$ photocatalytic reduction under the optimal experimental conditions. Photoinduced electrons are the major reductive substance of $Cr^{6+}$, and the mechanism involves adsorption of $HCrO_4^-$, reduction of $Cr^{6+}$, and desorption of $Cr^{3+}$. The $TiO_2$ photocatalyst has a reliable lifespan for reduction $Cr^{6+}$ under visible light irradiation and its

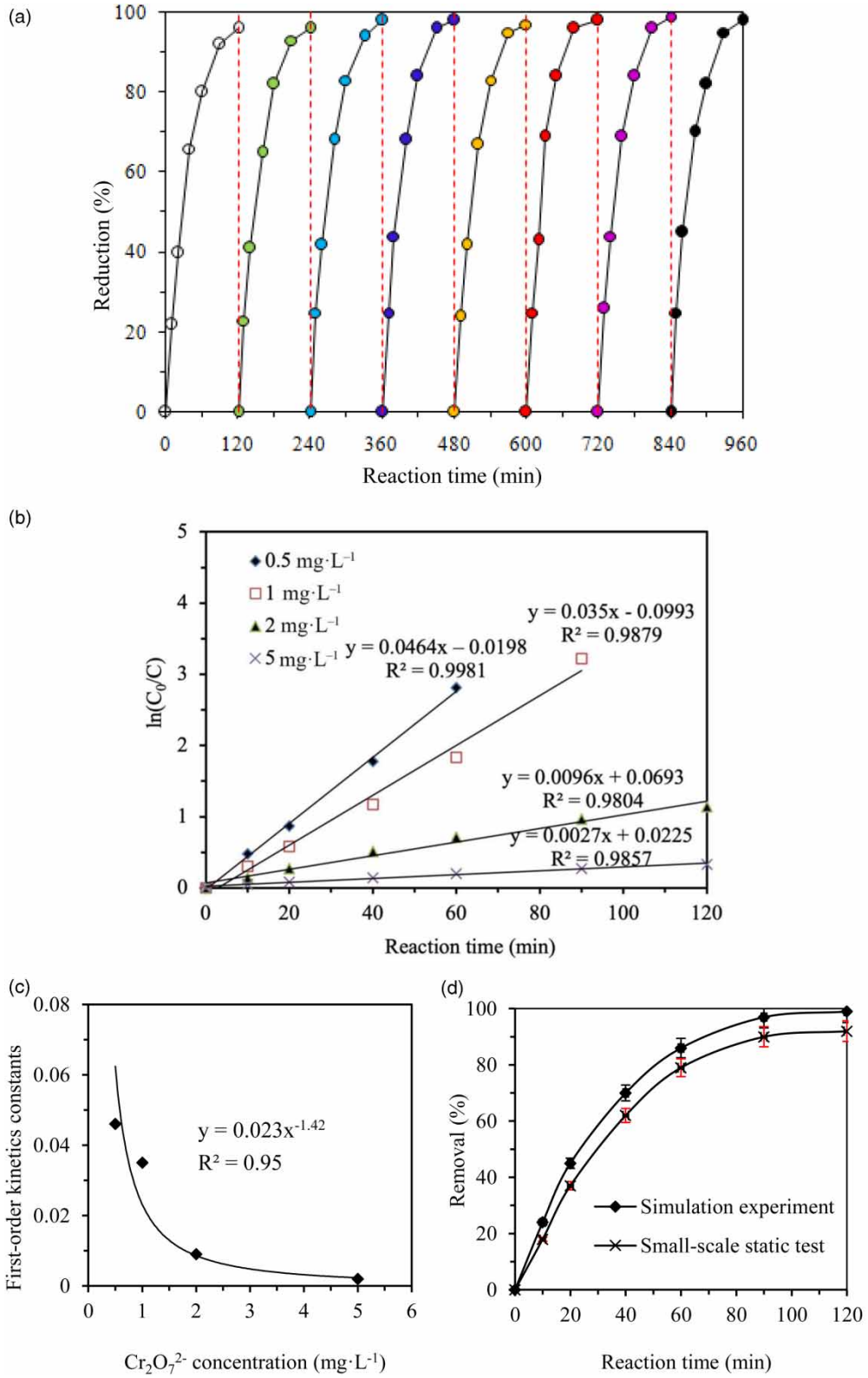


**Figure 6** | (a) Life span of $TiO_2$ photocatalyst of $Cr^{6+}$; (b) relationship between ln ($C_0$/C) and reaction time; (c) effect of $Cr_2O_7^{2-}$ initial concentration on first-order kinetics constants; (d) removal of $Cr^{6+}$ in simulation experiment and small-scale static test under the same experiment conditions.

**Table 1** | Properties of wastewater

| $Cr_2O_7^{2-}$ | pH | Turbidity | Temp. | Conductivity | $Ca^{2+}$ | $Na^{+}$ | $NO_3^{-}$ | $Cl^{-}$ |
|---|---|---|---|---|---|---|---|---|
| $1\ mg{\cdot}L^{-1}$ | 5 | 4 | 20 °C | $160\ m{\cdot}sm^{-1}$ | $10^{-3}\ mg{\cdot}L^{-1}$ | $10^{-3}\ mg{\cdot}L^{-1}$ | $10^{-3}\ mg{\cdot}L^{-1}$ | $10^{-3}\ mg{\cdot}L^{-1}$ |

photocatalytic reduction reaction fits well with pseudo-first-order kinetics.

## ACKNOWLEDGEMENTS

This work is economically funded by Natural Science Foundation of Shandong Province (No: ZR2019MEE097; ZR2016EEM15) and the National Water Pollution Control and Treatment Science and Technology Major Project (No: 2017ZX07101-002-05). Furthermore, we thank Colin Zhao for the revision in English grammar and sentences structure.

## DATA AVAILABILITY STATEMENT

All relevant data are included in the paper or its Supplementary Information.

## REFERENCES

Acharya, R., Naik, B. & Parida, K. 2018 Cr(VI) remediation from aqueous environment through modified-$TiO_2$-mediated photocatalytic reduction. *Beilstein Journal of Nanotechnology* **9**, 1448–1470.

Asgari, E., Sheikhmohammadi, A., Nourmoradi, H., Nazari, S. & Aghanaghad, M. 2021 Degradation of ciprofloxacin by photocatalytic ozonation process under irradiation with UVA: comparative study, performance and mechanism. *Process Safety & Environmental Protection* **147**, 356–366.

Ayub, S., Siddique, A. A., Khursheed, M. S., Zarei, A., Alam, I., Asgari, E. & Changani, F. 2020 Removal of heavy metals (Cr, Cu and Zn) from electroplating wastewater by electrocoagulation and adsorption processes. *Desalination & Water Treatment* **179**, 263–271.

Chatterjee, D. & Dasgupta, S. 2005 Visible light induced photocatalytic degradation of organic pollutants. *Journal of Photochemistry and Photobiology C: Photochemistry Reviews C* **6** (2–3), 186–205.

Deveci, H. & Kar, Y. 2013 Adsorption of hexavalent chromium from aqueous solutions by bio-chars obtained during biomass pyrolysis. *Journal of Industrial & Engineering Chemistry* **19** (1), 190–196.

Fujishima, A., Zhang, X. T. & Tryk, D. A. 2008 $TiO_2$ photocatalysis and related surface phenomena. *Surface Science Reports* **63** (11), 515–582.

Gheju, M. & Balcu, I. 2017 Assisted green remediation of chromium pollution. *Journal of Environmental Management* **203**, 920–924.

Gong, Y., Gai, L., Tang, J., Fu, J., Wang, Q. & Zeng, E. Y. 2017 Reduction of Cr(VI) in simulated groundwater by FeS-coated iron magnetic nanoparticles. *Science of the Total Environment* **595**, 743–751.

Gumy, D., Morais, C., Bowen, P., Pulgarin, C., Giraldo, S., Hajdu, R. & Kiwi, J. 2006 Catalytic activity of commercial of $TiO_2$ powders for the abatement of the bacteria (*E. coli*) under solar simulated light: influence of theisoelectric point. *Applied Catalysis B Environmental* **63** (1–2), 76–84.

Guo, S. H., Liu, Z. L., Li, Q. S., Yang, P., Wang, L. L., He, B. Y., Xu, Z. M., Ye, J. S. & Zeng, E. Y. 2016 Leaching heavy metals from the surface soil of reclaimed tidal flat by alternating seawater inundation and air drying. *Chemosphere* **157**, 262–270.

Habibi, S., Nematollahzadeh, A. & Mousavi, S. A. 2015 Nano-scale modification of polysulfone membrane matrix and the surface for the separation of chromium ions from water. *Chemical Engineering Journal* **267**, 306–316.

Hoffmann, M., Martin, S. T., Chio, W. & Bahnemann, D. W. 1995 Environmental applications of semiconductor photocatalysis. *Chemical Reviews* **95**, 69–96.

Jobby, R., Jha, P., Yadav, A. K. & Desai, N. 2018 Biosorption and biotransformation of hexavalent chromium [Cr(VI)]: a comprehensive review. *Chemosphere* **207**, 255–266.

Kerkez-Kuyumcu, Ö., Kibar, E., Dayıoğlu, K., Gedik, F., Özkara-Aydınoğlu, Ş., Gedik, F., Akın, A. N. & Zkara-Aydınoglu, S. Ö. 2015 A comparative study for removal of different dyes over M/$TiO_2$ (M = Cu, Ni, Co, Fe, Mn and Cr) photocatalysts under visible light irradiation. *Journal of Photochemistry & Photobiology A Chemistry* **311**, 176–185.

Magadevan, D., Dhivya, E., Mundari, N. D. A., Mishra, T. & Aman, N. 2019 Development of novel $TiO_2$-$Cu_2(OH)PO_4$ heterojunction as nanophotocatalyst for improved Cr(VI) reduction. *Journal of Environmental Chemical Engineering* **7** (2), 102968.

Ravindra, K. & Mor, S. 2019 Distribution and health risk assessment of arsenic and selected heavy metals in groundwater of Chandigarh, India. *Environ. Environmental Pollution* **250**, 820–830.

Sarahney, H., Mao, X. & Alshawabkeh, A. N. 2012 The role of iron anode oxidation on transformation of chromium by electrolysis. *Electrochimica Acta* **86**, 96–101.

Sheikhmohammadi, A., Mohseni, S. M., Hashemzadeh, B., Asgari, E., Sharafkhani, R., Sardar, M., Sarkhosh, M. & Almasiane, M. 2019 Fabrication of magnetic graphene oxide

nanocomposites functionalized with a novel chelating ligand for the removal of Cr(VI): modeling, optimization, and adsorption studies. *Desalination & Water Treatment* **160**, 297–307.

Testa, J. J., Grela, M. A. & Litter, M. I. 2004 Heterogeneous photocatalytic reduction of chromium(VI) over $TiO_2$ particles in the presence of oxalate: involvement of Cr(V) species. *Environmental Science & Technology* **38** (5), 1589–1594.

Vendruscolo, F., Ferreira, R. G. L. & Filho, N. R. A. 2017 Biosorption of hexavalent chromium by microorganisms. *International Biodeterioration & Biodegradation* **119**, 87–95.

Wang, Q., Yang, C., Hang, G. Z., Hu, L. & Wang, P. 2017 Photocatalytic Fe-doped $TiO_2$/PSF composite UF membranes: characterization and performance on BPA removal under visible-light irradiation. *Chemical Engineering Journal* **319**, 39–47.

Wang, X., Fu, R., Li, H., Zhang, Y., Xiong, Y., Lu, M., Xiao, K., Zhang, X., Zheng, C. & Xiong, Y. 2020 Heavy metal contamination in surface sediments: a comprehensive, large-scale evaluation for the Bohai Sea, China. *Environmental Pollution* **260**, 113986.

Wang, X., Zhang, L., Bu, Y. & Sun, W. 2021 Interplay between invasive single atom Pt and native oxygen vacancy in anatase $TiO_2$ (101) surface: a theoretical study. *Applied Surface Science* **540**, 148357.

Wu, Q., Zhao, J., Qin, G., Wang, C., Tong, X. & Xue, S. 2013 Photocatalytic reduction of Cr(VI) with $TiO_2$ film under visible light. *Applied Catalysis B Environmental* **142–143**, 142–148.

Xu, L., Bai, X., Guo, L., Yang, S. & Yang, L. 2019 Facial fabrication of carbon quantum dots (CDs)-modified N-$TiO_{2-x}$ nanocomposite for the efficient photoreduction of Cr(VI) under visible light. *Chemical Engineering Journal* **357**, 473–486.

Yang, S., Zhu, W., Jiang, Z., Chen, Z. & Wang, J. 2006 The surface properties and the activities in catalytic wet air oxidation over $CeO_2$–$TiO_2$ catalysts. *Applied Surface Science* **252** (24), 8499–8505.

Yang, Q., Li, Z., Lu, X., Duan, Q., Huang, L. & Bi, J. 2018 A review of soil heavy metal pollution from industrial and agricultural regions in China: pollution and risk assessment. *Science of the Total Environment* **642**, 690–700.

Yao, W., Wang, J., Wang, P., Wang, X., Yu, S., Zou, Y., Hou, J., Hou, J., Hayat, T., Alsaedi, A. & Wang, X. 2017 Synergistic coagulation of GO and secondary adsorption of heavy metal ions on Ca/Al layered double hydroxides. *Environmental Pollution* **229**, 827–836.

Yoshinaga, M., Ninomiya, H., Al Hossain, M. M. A., Sudo, M., Akhand, A. A., Ahsan, N., Alim, M. A., Khalequzzaman, M., Iida, M., Yajima, I., Ohgami, I. N. & Kato, M. 2018 A comprehensive study including monitoring, assessment of health effects and development of a remediation method for chromium pollution. *Chemosphere* **201**, 667–675.

Yu, X., Yu, R. Q., Gui, D., Zhang, X. & Wu, Y. 2018 Hexavalent chromium induces oxidative stress and mitochondria-mediated apoptosis in isolated skin fibroblasts of Indo-Pacific humpback dolphin. *Aquatic Toxicology* **203**, 179–186.

Zhang, C., Xia, F., Long, J. & Peng, B. 2017 The pollution of chromium in wet-end process of leather manufacture. *Journal of Cleaner Production* **154**, 276–283.

Zhao, B., Lv, M. & Zhou, L. 2012 Photocatalytic degradation of perfluorooctanoic acid with beta-$Ga_2O_3$ in anoxic aqueous solution. *Journal of Environmental Science* **24** (4), 774–780.

Zhao, B., Li, X., Li, W., Yang, L., Li, J., Xia, W., Zhou, L. & Zhao, C. 2015 Degradation of trichloroacetic acid by an efficient Fenton/UV/$TiO_2$ hybrid process and investigation of synergetic effect. *Chemical Engineering Journal* **273**, 527–533.

Zhao, B., Wang, X., Shang, H., Li, X., Li, W., Li, J., Xia, W., Zhou, L. & Zhao, C. 2016 Degradation of trichloroacetic acid with an efficient Fenton assisted $TiO_2$ photocatalytic hybrid process: reaction kinetics, byproducts and mechanism. *Chemical Engineering Journal* **289**, 319–329.

Zhou, X., Korenaga, T., Takahashi, T., Moriwake, T. & Shinoda, S. 1993 A process monitoring/controlling system for the treatment of wastewater containing chromium (VI). *Water Research* **27** (6), 1049–1054.

First received 29 December 2020; accepted in revised form 14 March 2021. Available online 26 March 2021